Use of three-dimensional computational fluid dynamics model for a new configuration of circular primary settling tank

A. G. Griborio, J. A. Rodríguez, L. Enriquez and J. A. McCorquodale

ABSTRACT

Appropriately used, computational fluid dynamics models are powerful tools to design and optimize primary settling tanks (PSTs). This paper uses a Fluent-based 3D model to identify the possible causes for underperformance of the circular PSTs at the Cali waste-water treatment plant, Colombia, and to propose design modifications to improve performance. A new configuration for the center well (CW) is proposed and evaluated. The influence of a rotational sludge scraper and of continuous sludge removal were considered in the numerical simulation. The new configuration included the modification of the current CW diameter and the location of a second baffle with the CW. The results suggest that the installation of the second baffle allows a more uniform flow distribution within the PST and consequently, the hydrodynamic problems associated with short-circuiting of the influent to the bottom of the tank are reduced. The second baffle suppresses the downward current, effectively dissipates the kinetic energy in the influent and forces the particles to move toward the bottom of the PST. In addition, the second CW baffle allows the formation in the inlet zone of a consistently more concentrated sludge blanket layer and thicker sludge, reducing the risk of solids leaving in the effluent of the PST.

Key words | center well, circular primary settling tank, computational fluid dynamics

A. G. Griborio (corresponding author)
Hazen and Sawyer,
P.C., 4000 Hollywood Blvd 750N, Hollywood,
FL 33021,
USA
E-mail: *agriborio@hazenandsawyer.com*

J. A. Rodríguez
L. Enriquez
EIDENAR, Faculty of Engineering,
University of Valle,
Cali,
Colombia

J. A. McCorquodale
Department of Civil Engineering,
University of New Orleans,
New Orleans,
LA 70122,
USA

HIGHLIGHTS

- Three-dimensional CFD model for the evaluation of a new configuration for a circular PST.
- The model includes the simulation of the sludge scraper movement by means of a sliding mesh.
- Optimization of circular PST performance.
- New configuration of center well for circular PST.
- Formation of a consistent more concentrated sludge blanket in circular PST.

INTRODUCTION

Primary settling tanks (PSTs) are typically used in a waste-water treatment plant (WWTP) to remove suspended solids from the influent raw wastewater. Since the PSTs are an initial step in the treatment, the efficiency of their operation influences the subsequent biological and sludge treatment units (Gernaey & Vanrolleghem 2001), as well as the biogas and electric energy production in systems with anaerobic digestion and cogeneration (Patziger *et al.* 2016). Consequently, PSTs strongly influence the efficiency of the entire wastewater treatment plant (Asgharzadeh *et al.* 2011; Patziger *et al.* 2016).

The design of PSTs is usually based on either surface overflow rate or hydraulic retention time (Droste 1997;

doi: 10.2166/wst.2021.110

Patziger & Kiss 2015) with the assumption of uniform velocity distribution over the depth and width of the tank. Typically, the particle velocities are treated as constant within specified mass fraction classes. These assumptions are not always realistic and may lead to design and performance problems (Tamayol *et al.* 2008). For example, the flow in real tanks is highly non-uniform and can result in 'dead' zones and short-circuiting which tend to reduce the removal efficiency. Density currents, due to influent suspended solids, have different effects on the flow patterns in primary and secondary settling tanks; consequently, the design of inlets and baffles will differ. The process of flocculation or floc breakup can change the settling velocities and/or the fraction in a specific class.

The prediction of sedimentation in a PST is challenging since many factors affect the capacity and performance of a PST: the fraction of non-settleable particles (typically exceeding 40% of the total influent concentration), floating particles (Abdel-Gawad & McCorquodale 1985; Li *et al.* 2008), the sludge rheology and density coupled with solids removal mechanism (Griborio *et al.* 2014) and the geometry of the tank, especially, the location of the inlet and outlet baffles (Razmi *et al.* 2009). Additionally, PSTs are characterized by recirculation zones, bottom currents, turbulence, density currents (Tamayol *et al.* 2008; Razmi *et al.* 2009) and thermal density currents induced by variable influent temperatures as well as surface heat exchange (Griborio *et al.* 2014). Therefore, short-circuiting and dead areas are created, which reduce the effective sedimentation volume of the PST and solids may be resuspended, affecting the performance of these tanks (Tamayol *et al.* 2008; Razmi *et al.* 2009).

Several mathematical models have been proposed to describe the behavior of PSTs. These models include 1D models, but because more information about the different phenomena and their interactions in the sedimentation tank are required to accurately predict the tank performance (Balemans 2014), 2D and 3D models, also referred to as Computational Fluid Dynamics (CFD) models (WEF 2005), have been developed. The 2D models can predict sedimentation tank performance but cannot resolve asymmetric flows and geometry effectively. In contrast, a 3D model can fully resolve geometry and complex phenomena that are non-symmetrical. This way, a 3D model can be confidently used to simulate non-symmetric influent configurations, swirl effects induced by rotating scrapers and inlet vanes, hydrodynamic circulation and turbulence issues, which are relevant for the accurate simulation of the flow field, beyond the capabilities of some 2D models (Gong *et al.* 2010). In the last decade, commercial CFD solution-codes, such as ANSYS FLUENT, have been widely used for 3D secondary settling tank (SST) and PST modeling due to their advantages of easy-learning, friendly interface, and stability (De Clercq 2003; Goula *et al.* 2008; Patziger *et al.* 2016; Zhang 2017; Gao & Stenstrom 2019).

Hazen (1904) provided what can be considered the earliest PST model. The Hazen model introduced the concept of surface overflow rate and the simulation of discrete settling that is typically expected to occur in PSTs; a uniform horizontal flow was assumed, and turbulence was neglected (WEF 2005). Although later studies tried to improve upon the Hazen model by applying vertical mixing and they were aware of the importance of turbulent mixing and recirculation zones (Dobbins 1944; Camp 1946; Tebbutt & Christoulas 1975; Alarie *et al.* 1980; Paraskevas *et al.* 1993), they were not able to provide adequate solutions due to the lack of suitable hydrodynamics and turbulence models (Stamou 1995; Tamayol & Firoozabadi 2006). Thus, advanced numerical models were developed to simulate a realistic non-uniform velocity profiles by including a classification of influent solids in which a nonsettleable class was considered (Abdel-Gawad & McCorquodale 1985; Stamou *et al.* 1989; Tarpagkou *et al.* 2013; Tarpagkou & Pantokratoras 2014; Bachis *et al.* 2015). Also, the effect of variations in flocculation state on the settling process was studied (Torfs *et al.* 2017). Moreover, for a better understanding of the flow pattern in both SST and PST, a k-ε turbulence model was developed and improved (Celik *et al.* 1985; Adams & Rodi 1990; Stamou 1991; Patziger & Kiss 2015; Das *et al.* 2016; Rodi 2017; Gao & Stenstrom 2018). In the same way, other models accounted for the density currents effects on particle settling as a result of both the suspended solids and temperature gradients in the settling tanks (Devantier & Larock 1986; Zhou *et al.* 1994; Goula *et al.* 2008; Kriss & Ghawi 2008).

Over the last three decades, CFD modeling has been extensively used to explore the flow pattern of rectangular PSTs and to optimize their design, but fewer studies have been carried out in circular PSTs (Liu & García 2007, 2011; Goula *et al.* 2008). The results obtained from all studies (rectangular and circular PSTs) suggest that inlet design of PSTs should focus on dissipating the kinetic energy or velocity head of the sewage, avoiding short-circuiting, alleviating the density currents effects and minimizing the blanket disturbances. One applicable method to reduce the volume of the dead zones and increase the performance of the sedimentation tanks is to use a proper baffle configuration. Therefore, various models have been developed to study the optimal position and size of the baffles for PSTs

(Tamayol & Firoozabadi 2006; Tamayol *et al.* 2008; Razmi *et al.* 2009; Liu & García 2011; Rostami *et al.* 2011; Shahrokhi *et al.* 2011, 2012, 2013; Esping *et al.* 2012; Zhang 2017). Furthermore, the inlet pipe arrangement, tank side water depth and feedwell depth have also been identified as important parameters affecting the PST behavior (Liu & García 2011). However, these models used relatively simple PST geometries and the solids removal was considered as an outlet for sludge on the tank floor; these simplifications do not reproduce some of the real behavior of PST. Furthermore, these models neglected the impact of the rotating scraper on sludge blanket height and on the tank hydrodynamics.

It can be concluded from the above referenced research that the current way in which circular PSTs are designed could and should be improved. Through the use of CFD as a tool that allows understanding, quantifying and visualizing the major processes dominating the tank performance, this research generated a new configuration that might lead to circular PST optimization. To achieve such an objective, field experiments and CFD modeling were conducted. The CFD model was developed for one of the circular PST located at the Cañaveralejo WWTP of Cali, Colombia. Additionally, the applied model included 3D geometry and the use of a rotational sludge scraper. Furthermore, the influence of continuously sludge removal is considered in the numerical simulation.

METHODS

The first objective of this research was to obtain, through mathematical modeling supported by field and laboratory data, a thorough understanding of the behavior of the PSTs found at the Cañaveralejo WWTP in Cali, Colombia. Accordingly, a CFD model was developed with the general components of good modeling practice (Wicklein *et al.* 2015): (1) clearly defining the objective of the modeling task with all project parties involved; (2) collection of data, defining the model configuration (mesh generation) and simulation settings; (3) running the simulations and (4) post-processing, calibration, and validation. The CFD model was developed to simulate and analyze the flow patterns and solid settling with the current PST configuration to identify the root cause of the apparent underperformance. The CFD package FLUENT 16.1 is used in this project as a modeling platform. Finally, a new configuration is proposed to improve the PST performance after evaluating different alternatives using the developed CFD model.

Geometry and meshing

DesignModeler, a 3D computer-aided design program included in ANSYS Workbench, was used to digitize the computational domain of a single PST of the Cañaveralejo WWTP, which has a rated capacity of 7.6 m^3/s. The Cañaveralejo WWTP has eight identical circular PSTs. Individual tank dimensions are: 47.5 m for internal diameter and 4.2 m for the side water depth.

Since the PSTs were identical, the modeling effort was confined to one PST. The CFD model included the major clarifier features and characteristics such as the influent column, the feedwell or center well (CW), the peripheral effluent weir, the sludge hopper, the rotational sludge scraper, and the sludge pipe.

After the geometry of the PST was generated, the computational domain was meshed into a finite number of grid cells. Great efforts, including sensitivity analyses, were dedicated to find a proper mesh. The mesh density was chosen such that the grid was finest where higher velocity gradients occur and where velocity is expected to have a greater impact on the sedimentation process. A mesh-independency study was performed to eliminate errors due to the coarseness of the grid and to determine the best compromise between simulation accuracy, numerical stability, convergence, and computational time. The mesh-independency was investigated by comparing grids with 373,360 (coarse), 500,252 (medium) and 644,428 (fine) elements of hexahedral form. A qualitative analysis of the velocity and volume fraction patterns, and a quantitative analysis of effluent total suspended solids (TSS) concentration were used to compare the three meshes. The simulation results with the medium mesh did not diverge significantly from the case with the fine mesh, but the difference between the prediction of the coarse mesh to other two meshes was significant and thus the medium mesh was selected.

The sludge scraper movement was incorporated into the model by means of a sliding mesh. To incorporate this approach, it was necessary to split the domain in two parts: stationary frame and rotatory frame, which are connected through an interface called the contact region.

The computational domain and its components as well as the mesh are presented in Figure 1. The scraper contact region is shown in green in the plan view.

Multi-phase model

Settling column tests were conducted during the initial experimental stage to identify the settling model to be used;

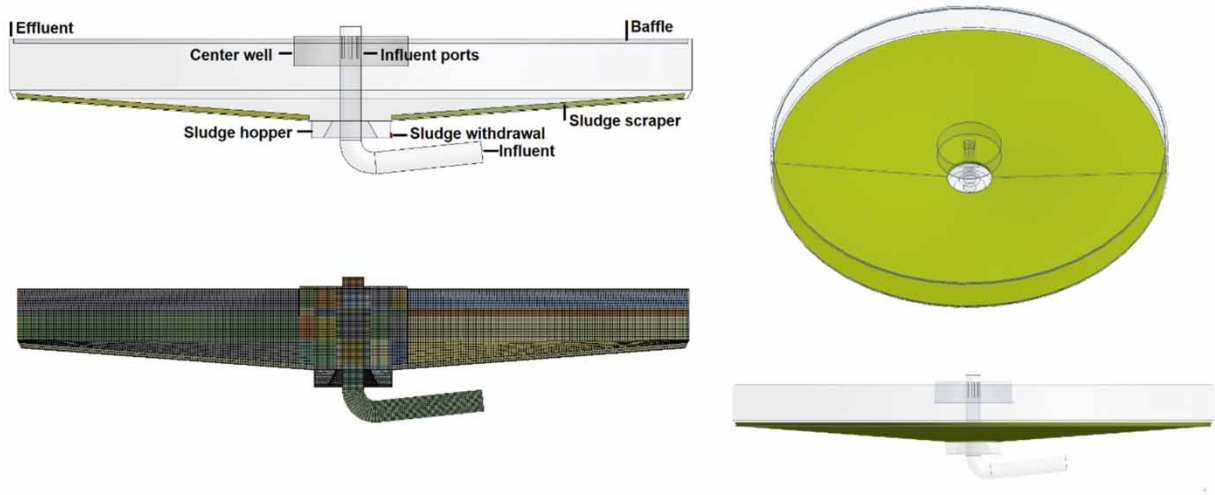

Figure 1 | 3D geometry and the mesh of original circular PST.

however, it was decided to take advantage of the two-phase model already available in the software ANSYS Fluent. In this study, a mixture model was used as the multi-phase model; this is an alternative to the commonly used Vesilind settling model. This model has successfully been used in the past to simulate fluids in sedimentation tanks (De Clercq 2003; Al-Sammarraee *et al.* 2009; Wicklein & Samstag 2009; Yeoh & Tu 2009; Liu & García 2011; Zhu *et al.* 2012; Zhang 2014; Samstag *et al.* 2016; Guo *et al.* 2017). The mixture model can be applied in flows for a wide range of velocity differences, particle sizes and densities as long as the force equilibrium is achieved (Manninen *et al.* 1996).

Based on the discretization of the measured particle size distribution while maintaining a sufficient but not excessive number of equations to solve, three secondary classes of solids were implemented in the mixture model each with a different particle size (10, 50 and 80 μm). The density of the secondary phase was 1,396.5 kg/m^3 and the properties of primary phase (water) were a density of 997.5 kg/m^3 and a viscosity of 0.000924 kg/m.s. The particle size distribution was measured during five different events with averages of 14.9, 56.4 and 28.7% for the 10, 50 and 80 μm particle sizes, respectively. These events are described in the calibration and validation section along with the calibration results. These results indicate that three classes are suitable to simulate with a high degree of accuracy the dynamic behavior of the Cañaveralejo PSTs.

Turbulence model

The purpose of choosing turbulence models is to find the most suitable model that fits the physical reality and gives reliable results. The computational cost in terms of CPU time and memory of the individual models was also considered. Gao & Stenstrom (2018) suggest that more observations inside the inlet zone are needed to achieve better model calibration and correct application of the turbulence model, which can be crucial to optimizing the geometry of the inlet structure and sludge hopper. Because of its robustness, economy and reasonable accuracy to better describe low Reynolds numbers flows in sedimentation tank, the standard k-ε model (SKE) was used to account for turbulence (Stamou *et al.* 1989; Zhou & McCorquodale 1992; Zhou *et al.* 1994; De Clercq 2003; Fan *et al.* 2007; Liu & García 2011; Stamou 2008; Gong *et al.* 2011; Shahrokhi *et al.* 2012, 2013; Ramin *et al.* 2014).

In sedimentation tanks, the hydraulic behavior near the wall can expect high gradient changes due to flow and particle collisions (Guo *et al.* 2017). Therefore, the near-wall region was modeled via standard semi-empirical logarithmic wall functions, which imposes the no slip boundary condition (Stamou 2008; Al-Sammarraee *et al.* 2009; Xanthos *et al.* 2011; Ghawi & Kriš 2012; Ramin *et al.* 2014; Guo *et al.* 2017).

Governing equation

The equations that govern the flow of an incompressible Newtonian fluid are unsteady Eulerian equations that describe the conservation of mass (continuity) and the momentum also known as the Navier–Stokes equation and energy equation. The details about the formulation could be found in ANSYS Fluent (ANSYS 2016). For closing the momentum equation, the standard k-ε model for

calculation of Reynolds stress is added to these equations (De Clercq 2003; Dufresne *et al.* 2009; Wang *et al.* 2010).

The standard k-ε model includes two major equations. These are turbulent kinetic energy equation (k) (Equation (1)), and equation of dissipation energy (ε) (Equation (2)) (ANSYS 2016):

$$\frac{\partial}{\partial t}(\rho k) + \frac{\partial}{\partial x_i}(\rho k u_i) = \frac{\partial}{\partial x_j}\left[\left(\mu + \frac{\mu_t}{\sigma_k}\right)\frac{\partial k}{\partial x_j}\right] + G_k + G_b - \rho\varepsilon - Y_M + S_k \quad (1)$$

$$\frac{\partial}{\partial t}(\rho \varepsilon) + \frac{\partial}{\partial x_i}(\rho \varepsilon u_i) = \frac{\partial}{\partial x_j}\left[\left(\mu + \frac{\mu_t}{\sigma_\varepsilon}\right)\frac{\partial \varepsilon}{\partial x_j}\right] + C_{1\varepsilon}\frac{\varepsilon}{k}(G_k + C_{3\varepsilon}G_b) - C_{2\varepsilon}\rho\frac{\varepsilon^2}{k} + S_\varepsilon \quad (2)$$

In these equations, Gb, Y_M and G_k are production terms of turbulence kinetic energy due to buoyancy, compressibility and mean velocity gradients, respectively. $C_{1\varepsilon} = 1.44$ and $C_{2\varepsilon} = 1.92$ are dimensionless empirical constants (Rodi 2017). $\sigma_k = 1$ and $\sigma_\varepsilon = 1.3$ are the turbulent Prandtl numbers (Stamou 1991; De Clercq 2003; Fan *et al.* 2007; Weiss *et al.* 2007; Amini *et al.* 2013; Ekmekçi 2015; Rodi 2017). Two source terms S_k and S_ε are used to take the effect of the sludge removal on k and ε into account (Weiss *et al.* 2007). The constant $C\mu$ used to define the turbulent (or eddy) viscosity μ_t was 0.09 (Weiss *et al.* 2007; Ekmekçi 2015; Rodi 2017).

Moreover, to include the high concentration of solid particles that leads to interparticle collisions (sludge blanket), the 'granular option' was selected in the mixture model. In this option, molecular cloud theory is applied to the particle phase. This theory leads to the appearance of additional stresses in momentum equations which are determined by intensity of particle velocity fluctuations (ANSYS 2016). Consequently, the equations proposed by Schaeffer (1987) and Gidaspow *et al.* (1992) were selected to describe granular and collisional viscosity and frictional viscosity, respectively. Additionally, to define solids pressure, the equation presented by Lun *et al.* (1984) was applied (Cloete *et al.* 2011, 2012; Klimanek *et al.* 2015; Cloete & Amini 2016; Zhou *et al.* 2016; Zhang *et al.* 2017). Within these formulations, the radial distribution function was calculated according to Ogawa *et al.* (1980) (Cloete *et al.* 2011; Zhou *et al.* 2016) and the packing limit value of 0.3 was used. Kinetic energy associated with particle velocity fluctuations was represented by a granular temperature and inelasticity of the granular phase.

The modeling of the rotating flow such as those found around or induced by the sludge scraper is important because of the effect it has on the hydraulic behavior of the sedimentation tank. One method of explicitly calculating the flow field in a rotating flow scenario is the sliding mesh method. The sliding grid model explicitly calculates the mixing region, and then rotates this section of the grid relative to the rest of the domain. It is assumed the flow field is unsteady, and the interactions are modeled as they occur (Bridgeman *et al.* 2009). Consequently, the sliding mesh model was used to simulate the rotating motion of sludge scraper, which is available in ANSYS Fluent as 'mesh motion option'. While the sliding mesh method is the most computationally demanding, it is also the most accurate method for simulating flows in multiple moving reference frames.

Numerical solution

The governing equations were numerically solved using the finite volume method. The segregated pressure-based solver for incompressible flows was selected (De Clercq 2003; Goula *et al.* 2008; Carbone *et al.* 2014; Roy *et al.* 2014; Patziger & Kiss 2015). The pressure and velocity were coupled using the SIMPLE algorithm. The spatial discretization schemes were body force weighted (pressure), second order upwind (momentum, turbulent kinetic energy and energy), least square cell based (gradient) and QUICK (volume fraction). Temporal discretization of the governing equations was performed by a first-order implicit scheme.

Because the governing equations are non-linear, the solution procedure is iterative. To achieve the convergence in the solutions, under-relaxation factors of 0.1 (slip velocity), 0.2 (granular temperature), 0.3 (momentum), 0.5 (volume fraction, turbulent kinetic energy and turbulent dissipation energy), 0.7 (pressure) and 1 (other variables) were adopted. Additionally, the convergence is indicated by the residual of key variants continuity, velocity components and turbulence parameters. The solution was considered converged when the normalized residual value for all variables was 10^{-3} (Ying & Sansalone 2011; Garofalo 2012; Yu *et al.* 2013; Rameshwaran *et al.* 2013). The time step selected was 3 s.

Boundary and initial conditions

Prior to performing simulations, the system was defined by a set of operational characteristics and boundary conditions. In the model, five different boundary types were defined. Unidirectional constant velocity is specified at the inlet

according to the flow rate and cross-section area of the inlet pipe. The flow rate and inlet velocity are presented in the following section. At the effluent weir (outlet) and sludge-withdrawal outlet, an outflow boundary condition is applied. For this type of boundary, no conditions need to be defined. Instead, all variables at the outlet are extrapolated from the computed variables in the cells near the outlet. The walls were configured as 'stationary walls' with the exception of those located in the moving area, which were configured as 'moving walls' and the 'no slip' option was selected.

The free water surface was considered as a symmetry plane where changes in the water surface positions are negligible. Additionally, the 'Symmetry' boundary condition assumes that there is no diffusion, so the normal velocity component and the normal gradients of all other variables are zero at the symmetry plane. Finally, the inlet turbulence boundary condition was specified using the estimated turbulence kinetic energy (TKE) (6.01×10^{-4} m^2/s^2) and turbulent dissipation rate (TDR) (3.6×10^{-5} m^2/s^3) (De Clercq 2003; Kim *et al.* 2005; Weiss *et al.* 2007; Razmi *et al.* 2009; Liu & García 2011; Kiss 2012; Shahrokhi *et al.* 2013; Balemans 2014; Cloete & Amini 2016).

RESULTS AND DISCUSSION

Calibration and validation

The CFD model was calibrated and validated using a comprehensive field data set collected at the Cañaveralejo WWTP. The field data collected include clarifier influent flow, (b) primary sludge flow, (c) influent and effluent TSS concentrations, (d) primary sludge concentrations, and (e) particle size distribution (PSD).

PSD was analyzed for the influent and effluent of the PST using a laser diffraction particle analyzer. The PSD results indicate a higher proportion of small particles in the effluent compared to the influent, indicating that the largest particles were basically removed during the sedimentation process. The simulation results using influent particle sizes of 10, 50 and 80 μm showed a high degree of agreement with the observed data.

The model was calibrated with data collected over a one-day period (Date 1) of the PST and was validated using additional data over a four-day period (Dates 2 to 5). A sensitivity test on particle sizes was conducted to select the best set of three particle diameters to represent the effluent concentration on Date 1. Data from the subsequent days were used for validation. During these dates, the influent flow rate to the PST was maintained basically constant at 1.27 ± 0.01 m^3/s (inlet velocity of 0.72 m/s). Even though some differences between the simulated and measured data were observed, the results presented in Table 1 revealed an acceptable agreement between the model and the field data both in terms of the prediction of effluent total suspended solids (ETSS) concentration and TSS efficiency. Note that the mean predictive errors in the ETSS and efficiency are less than typical errors reported by De Clercq (2003), McCorquodale *et al.* (2005), Fan *et al.* (2007) and Patel *et al.* (2016). Based on these verifications, the model was considered to possess reasonable predictive capability and suitable for application.

New PST configuration

The nature of flow in the inlet is of critical importance to the PST performance, since it is generally here that most of the aggregation and energy dissipation process occurs (Griborio & McCorquodale 2006; Goula *et al.* 2008; Applegate *et al.* 2010; Ghawi & Kriš 2011; Liu & García 2011; Shahrokhi *et al.* 2012; Zhu *et al.* 2012; Das *et al.* 2016). The flow inside the CW is turbulent, having an influence on the particle aggregation process and consequently the size and density of aggregates that are formed, as well on the sedimentation process. Accordingly, the inlet zone should be designed to

Table 1 | Verification of ETSS concentration and efficiency

		ETSS concentration (mg/L)			Efficiency SST (%)		
Date	Influent concentration (mg/L)	Measured	Predicted	Error (%)	Measured	Predicted	Error (%)
1	160	60	68	13.3	62.5	57.5	−8.0
2	143	65	59	−9.2	54.5	58.7	7.7
3	132	68	63	−7.4	48.5	52.3	7.8
4	146	63	69	9.5	56.8	52.7	−7.2
5	150	72	68	−5.6	52.0	54.7	5.1

dissipate the kinetic energy of the influent; to provide a uniform radial flow pattern to maximize the use of the available settling area and to avoid inducing recirculation patterns in the bulk of the PST; to cope with variations in the flow rate or solids concentrations; and to be cost effective, easy to manufacture and retrofit (Nguyen *et al.* 2012).

Griborio & McCorquodale (2006) reported that the CW promotes the aggregation of unflocculated particles which has a major effect on the clarifier performance. However, an even greater benefit of the CW is the improvement of the tank hydrodynamics by reducing the strength of entrainment and recirculation flows. An important difference between the functioning of the inlet zone in PSTs and SSTs is that concentration-induced density currents are less important in PSTs which affect the design of the inlet and CW. For example, the downward deflection of the influent jets is less pronounced in PSTs than in SSTs which significantly changes the impact on the CW wall. The proposed new configuration of PST takes advantage of the weakness of the density effect in PSTs.

Based on these understandings, different geometrical configurations were modeled in this study to select the one that could be used to effectively enhance the hydraulic and sedimentation efficiency. The proposed geometrical configurations included the modification of CW diameter, the width of influent ports and the location of a second baffle within the CW. This second CW baffle (also referred to as second center well) was placed inside of the first CW to avoid a very strong downward current toward the sludge blanket and sludge hopper. The best arrangement is showed in Figure 2.

Velocity vectors and velocity contours

The results are focused on three different zones, identified as the main zones to establish the PST hydraulic behavior: feedpipe, inlet region and slope (outside of the hopper) and sludge hopper. Considering the relevance of hydrodynamic behavior in the PST efficiency, a detailed analysis of the velocity vectors and contours predicted by the model was carried out, to identify whether the modifications made are likely to reduce the hydrodynamic limitations identified in the original PST (OPST).

Velocity vector profile of the feedpipe and inlet ports are presented in Figure 3. This figure demonstrates the influence of the duct curvature on the flow, with the presence of the bend causing a non-uniform distribution of the mean velocity in its vicinity and influent ports. Njobuenwu *et al.* (2013) showed that changes in the direction of a flow, as in a bend, generate velocity and pressure gradients with strong shear layers close to the geometry boundaries. As a result, a higher velocity inlet on the left side of OPST is observed. However, even though this event also occurs in the NPST (Figure 3(b)), it can be observed that the flow pattern of both left and right side of PST is almost similar after the flow leaves the inlet ports. This suggests that the installation of the second CW baffle permits a uniform flow distribution among the PST and consequently, the hydrodynamic problems associated with short-circuiting of the influent to the bottom of the tank should be reduced.

Figure 4(a) displays that on both sides of OPST the horizontal influent hits the CW and immediately turns downward. The downward current is forced in the opposite direction to form a larger recirculation zone below the inlets port. Although the recirculation zones at both sides of the inlet zone are similar in rotation, on the left side the recirculation zone invades the near-field zone above the sludge hopper. Then, the current splits up at the bottom PST, and part of the current is directed towards the hopper. The other part of the current changes its direction and flows as a horizontal bottom current outside the inlet zone.

On the right side of OPST the current exits the recirculation zone and flows as a horizontal current from the bottom lip of the CW outside the inlet zone. Also, an

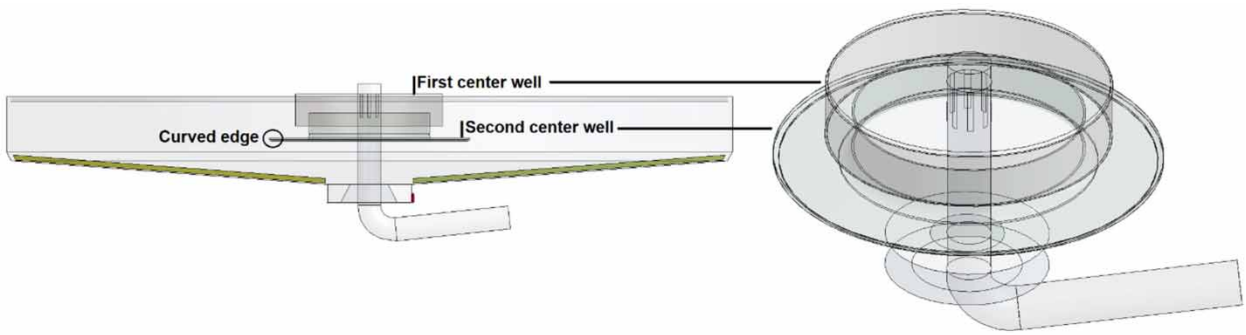

Figure 2 | New configuration of PST (NPST).

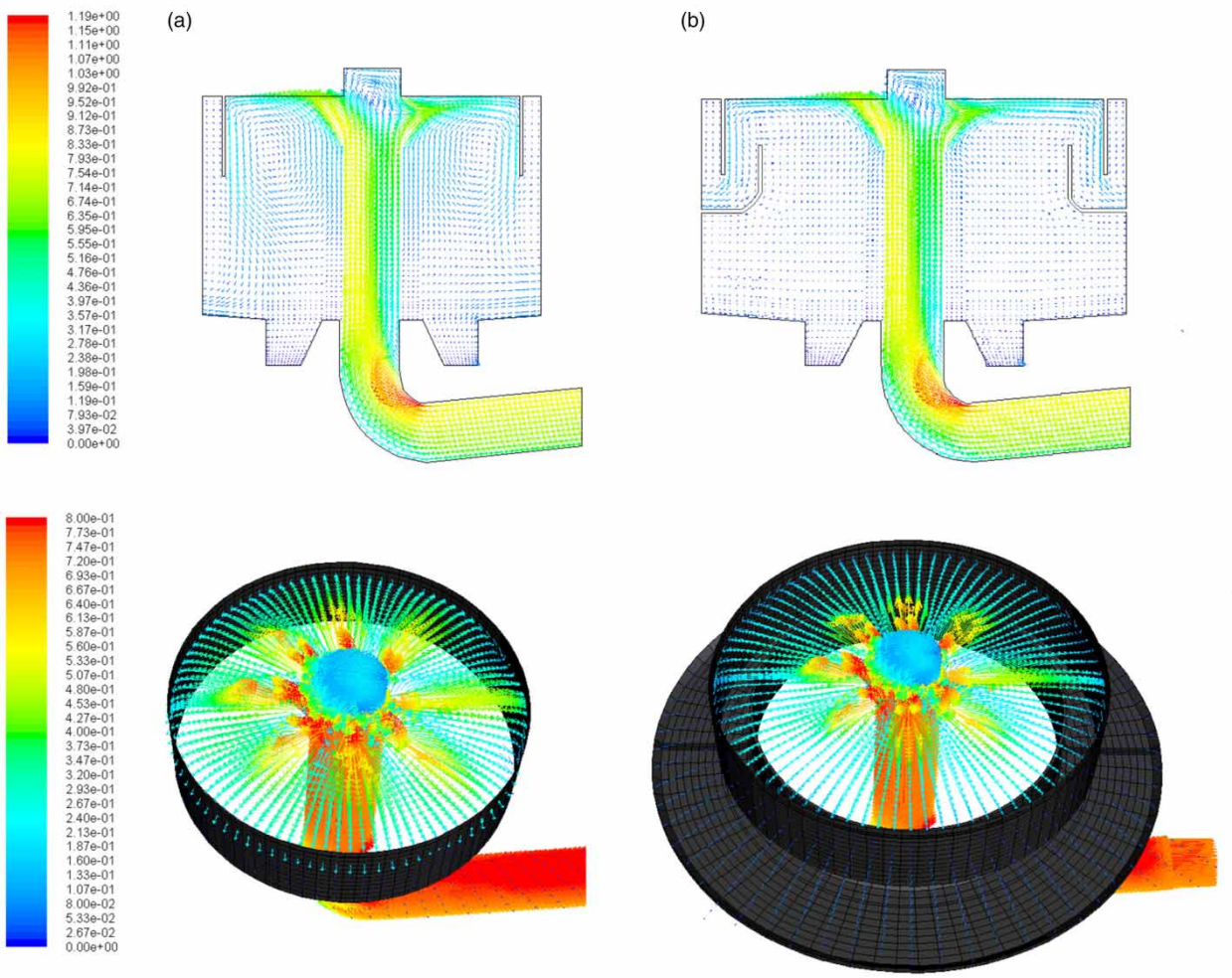

Figure 3 | Velocity vector (m/s) in feedpipe and inlet ports (a) OPST and (b) NPST.

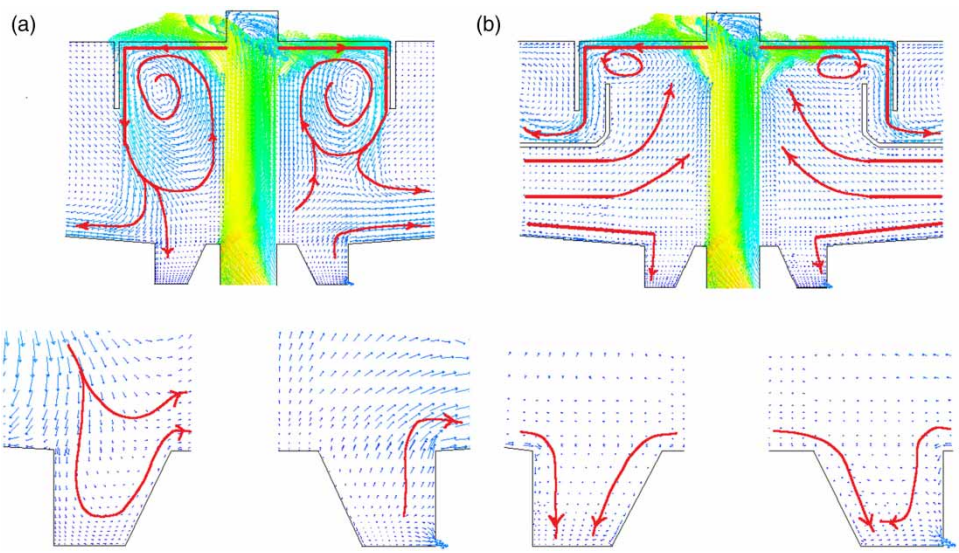

Figure 4 | Velocity vectors in inlet zone and sludge hopper (a) OPST and (b) NPST.

upward current is formed in the bottom hopper; this current travels over the hopper by running underneath the recirculation zone towards outside the inlet zone. Figure 4(b) shows that the flow patterns in the CW and hopper are significantly improved by the NPST.

After the horizontal current exits the inlet zone a second recirculation zone is formed at the near-field of sludge hopper (Figure 5(a)); this produces an upward current (similar in both sides). Additionally, the horizontal bottom current is still present and flows towards the peripheral wall in opposite direction to the flow induced by the scraper movement, which can potentially impact the scraper torque and efficiency. The NPST corrects these problems as indicated in Figure 5(b).

These findings suggest that the OPST efficiency is deteriorated by accumulation of settled solids in the slope (outside of the CW) and resuspension of settled solids, particularly in the sludge hopper. Thus, the solids transport toward the sludge hopper is compromised and may result in low withdraw sludge concentrations.

Otherwise, as shown in Figure 4(b), a recirculation zone in the inlet zone of NPST was identified but at a smaller magnitude than that found in the OPST. The influent flow turns sharply upward as a current reaching the zone between the first and second CW baffles and largest portion of the currents from the inlet ports is directed radially outward and not directed toward the PST bottom. Consequently, the recirculation in the inlet zone is reduced and the scouring on the thickened sludge at the sludge hopper is prevented.

A higher re-entrainment of flow from outside of the CW into the inlet zone is observed accompanied by two additional recirculation zones (counter-rotating eddies). This may promote contact between the suspended particles and provide favorable conditions for the settling process.

Furthermore, with the installation of the second CW baffle and especially by the curved edge of this CW, recirculation regions are formed behind the first CW (Figure 5(b)). This recirculation pattern avoids short-circuiting of influent to the effluent weir. The combination of the recirculation flow and small velocities appear to provide the required quiescent flow conditions for the settling process of the suspended solids.

According to Figure 5(b), the flow is forced upward and redirected back to the PST bottom. When the flow hits the bottom, it splits up into two opposite-direction currents, one bottom current towards the peripheral wall (first current) and other one towards the sludge hopper (second current). The fact that the direction of the second current is in the direction of the current induced by the scraper movement, and that the first current is weak and far from the hopper, provides a favorable condition for the settled solids to be directed towards the sludge hopper. This also prevents the settled solids from staying on the slope or accumulate in the corners.

The first current flows along the bottom of the end wall and then turns upwards to effluent weir. Over this current, a third current is developed which is directed towards the effluent weir.

The velocity contours shown in Figure 6(a) and 6(b) reveal the high impact that the inlet has on PST behavior. In the case of OPST, a marked downward velocity contour travels from the CW to the PST bottom closely approaching the sludge hopper. This results in elevating the sludge blanket and dragging solids outside the hopper. In the NPST, at the zone between the first CW and second CW, the inflow

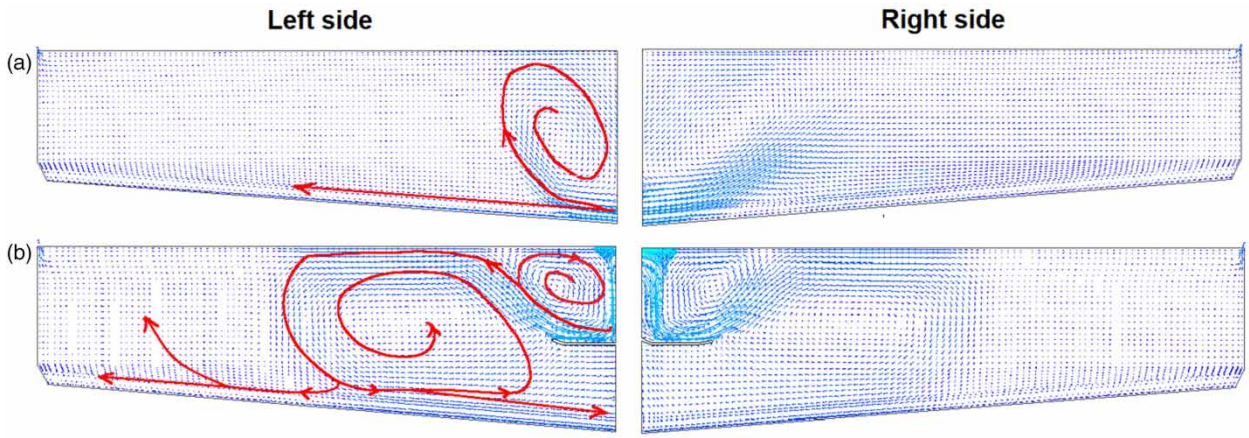

Figure 5 | Velocity vectors in clarification and slope zone (outside of CW): (a) OPST and (b) NPST.

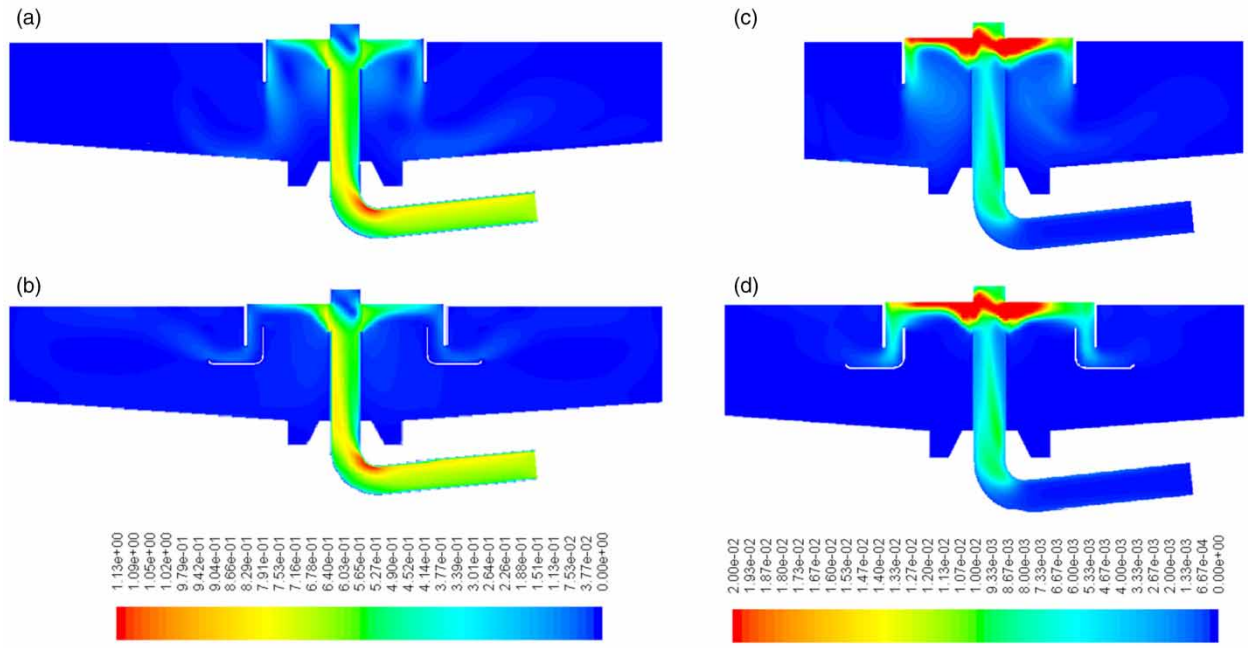

Figure 6 | Velocity contours (m/s) (a) OPST and (b) NPST and contour of turbulence kinetic energy (m^2/s^2) (c) OPST and (d) NPST.

energy is dissipated (Figure 6(d)) and the downward velocity is significantly reduced minimizing the impact on the sludge blanket. This flow pattern allows a higher solids concentration in inlet zone close to the sludge hopper (Figure 7). Outside of the inlet zone, the velocity magnitude is reduced gradually along the radial direction as the energy is dissipated.

As displayed in Figure 6(c) and 6(d), the turbulent kinetic energy is maximum at the inlet ports. The turbulent energy is confined and spread on the top of CW. Behind the CW, there is very low turbulence.

In a PST, an efficient CW is one that dissipates the initial kinetic energy to reduce solids dispersion (due to the relatively low suspended solid concentration), reduces entrainment and produces a radially uniform discharge flow at the CW exit. However, in the case of OPST no evidence of this was observed.

In NPST, at the zone between first CW and second CW, the TKE is still present, as the bulk of the flow currents pass through this region. Due to this, the inlet TKE will be fully dispersed and will not appear in the bottom current, therefore, short-circuiting is reduced in this region (Zhou & McCorquodale 1992). This indicates that when comparing the efficacy of OPST and NPST in dissipating the kinetic energy, the installation of second CW produces a better effect.

Sedimentation behavior

The density difference between a heavy fluid zone and a lighter fluid zone causes a stable density stratification (Gao & Stenstrom 2017) which contributes to a damping of vertical mixing (Samstag *et al.* 1992). When this happens, the density currents do not significantly affect the ETSS removal efficiency unless short-circuiting occurs and the upward currents flow directly to the exit (Gao & Stenstrom 2017). Consequently, as mentioned by several authors, because of the relatively low suspended solid concentration in PST, discrete particle settling prevails and the presence of solids does not greatly affect the flow pattern of the liquid but the mixture turbulence can be affected (Imam *et al.* 1983; Stamou *et al.* 1989; Liu & García 2011; Zhang 2017). Thus, in inlet zone of PST the concentration of the solids is required, and shear is needed to promote aggregation and to improve sedimentation process. Additionally, the inlet kinetic and potential energy must be satisfactorily dissipated within the inlet zone, which requires a design heavily based on hydrodynamic principles (satisfying volume and hydraulic retention time as well as optimal geometric design) (Patziger & Kiss 2015). In that respect, Figure 7 shows that unlike OPST, in the NSPT inlet zone a higher concentration of solids and sludge accumulation in the hopper were observed.

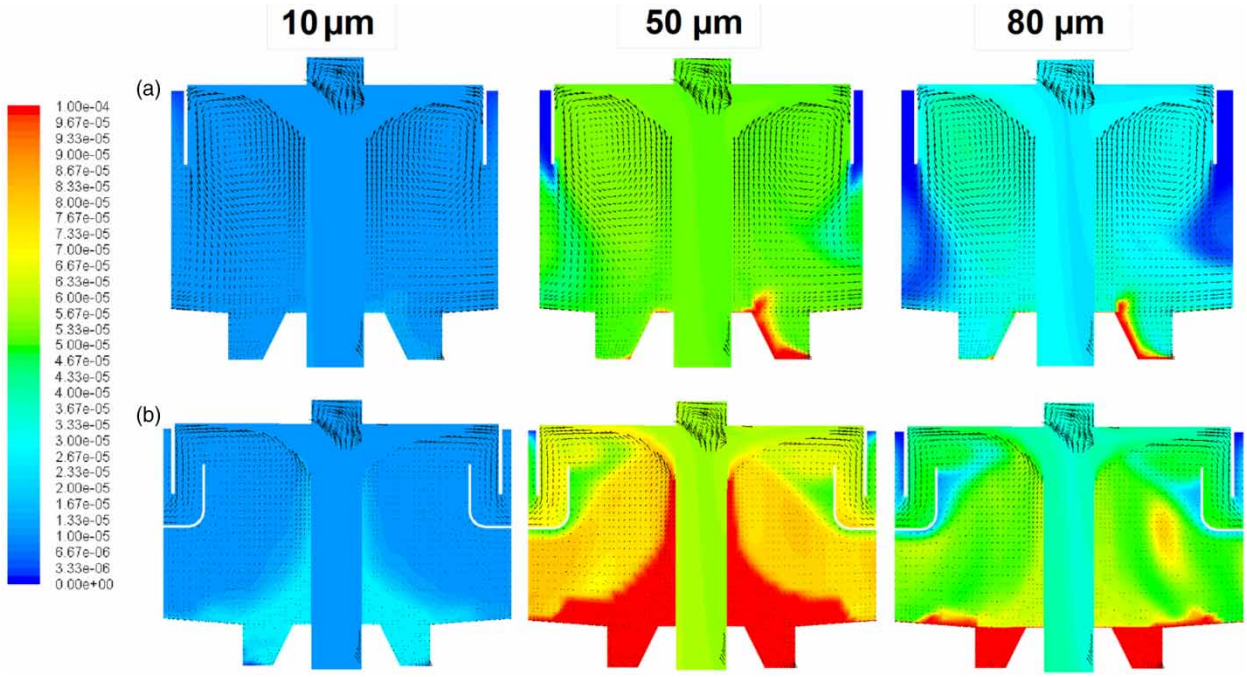

Figure 7 | Solid volume fraction in inlet zone and sludge hopper (a) OPST and (b) NPST. *Note*: The solids concentration can be obtained by multiplying the solids volume fraction by the density of the solids (1,396.5 kg/m^3).

According to the results shown in Figure 8, the particle size had a significant effect on the sedimentation efficiency. Particles of 80 µm displayed a satisfactory settling performance, and most of these particles settled to the slope bottom (OPST) or to the sludge hopper (NPST) (Figure 8(c)). However, the behavior of particles of 50 µm was diverse. A fraction of these particles became suspended in the flow field by the recirculation zone behind the first CW (in OPST) and second CW (in NPST), while others escaped into the outlet flow (Figure 8(b)).

In NPST, particles of 80 µm and 50 µm were prone to back mixing due to the recirculation zones and upward flow, eventually returning to the inlet zone and hopper. This event led to sludge accumulation at the hopper, consequently a higher sludge concentration in hopper was obtained and better sludge-withdrawal efficiency can be expected (Zhou *et al.* 2005). Unlike OPST where sludge accumulation at the slope bottom was observed, even though this sludge accumulation was high, its movement to the hopper was not fully achieved. Therefore, the sludge

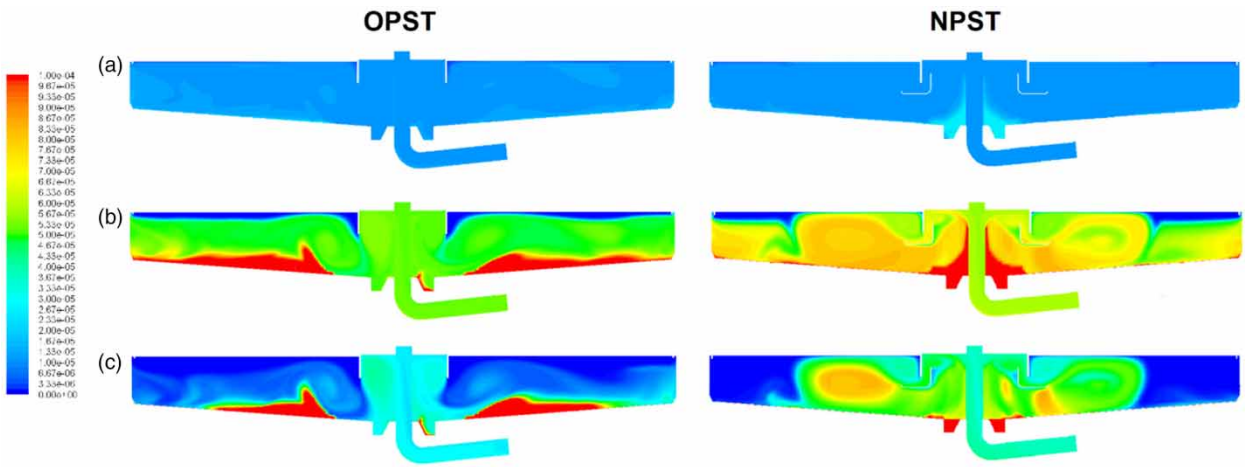

Figure 8 | Solid volume fraction (a) 10 µm; (b) 50 µm and (c) 80 µm.

withdrawal concentration was low and, over time, a major fraction of accumulated solids is expected to reach the tank outlet, affecting the sedimentation efficiency.

Otherwise, particles of 10 μm tend to come out with the effluent because of their small diameter and low settling velocity. Thus, the removal efficiency of these particles was almost zero (OPST) or lower than that of larger particles (NPST) (Figure 8(a)). However, a difference is observed between both PSTs, which consists of the ability to accumulate a fraction of these particles in the NPST hopper (Figure 7(b)).

Notice that in NPST the sludge inventory is observed as a sludge blanket and an accumulation of a thick sludge at the hopper, unlike OPST where the sludge inventory is observed as an accumulation on the slope bottom (Figures 7 and 8). This implies that the second CW of NPST allows the formation of a consistently more concentrated sludge blanket layer and promotes the accumulation and thickening of sludge in the hopper, reducing the risk of solids leaving the PST outlet.

To compare the performance between OPST and NPST, TSS concentration and efficiency are assessed (Table 2). It is apparent that in NPST the efficiency of the TSS removal is better than in the case of OPST by 8%. The advantage of the NPST configuration is also evident when the sludge-withdrawal concentration is evaluated. The OPST results in a diluted concentration because of the hydrodynamic limitations observed for this configuration. The NPST produces a thickened primary sludge with a high TSS concentration.

The results in Table 2 are presented for the calibration influent flow rate of 1.27 m^3/s, which is equivalent to a surface overflow rate of 61.92 $m^3/m^2/d$. While this surface overflow rate is typical for primary clarifiers, it is recommended that that the removal efficiency, sludge-withdrawal sludge concentration, and overall tank hydrodynamics of NPST are evaluated for different influent flow rates to determine the advantages of this configuration at different influent conditions.

Table 2 | Simulation results of the OPST and NPST

Flow Rate	OPST	NPST
Influent Flow Rate (m^3/s)	1.27	1.27
TSS Concentration	**OPST**	**NPST**
Inlet (mg/L)	160.0	160.0
Outlet (mg/L)	68.2	55.4
Efficiency (%)	57.4	65.4
Sludge withdrawal (mg/L)	994	28,410
10 μm Outlet (mg/L)	25.2	24.3
50 μm Outlet (mg/L)	41.4	31.0
80 μm Outlet (mg/L)	1.6	0.1

CONCLUSION

A 3D CFD model has been applied in this study to investigate and improve the performance of PST. Based on the CFD analysis of the OPST, a second CW baffle was proposed (NPST). The second CW baffle has been found to result in an improvement in PST performance with a more even distribution and symmetrical flow pattern.

In general, the second CW appears to provide better hydraulic behavior that than in the OPST, thus enhancing sedimentation. The second CW acts as an obstacle to suppress the downward current since influent TKE is effectively dissipated and forces the particles to move toward the bottom of the PST. In addition, the second CW allows, in the inlet zone, the formation of a consistently more concentrated sludge blanket layer and promotes the accumulation and thickening of sludge in the hopper, reducing the risk of solids leaving the PST outlet. The main advantage of second CW baffle lies in its ability to generate a thicker sludge. The second CW baffle could be easily installed in an existing PST as a solution to dilute sludge-withdrawal problems at minimal cost compared to other solution.

DATA AVAILABILITY STATEMENT

All relevant data are included in the paper or its Supplementary Information.

REFERENCES

Abdel-Gawad, S. M. & McCorquodale, J. A. 1985 Simulation of particle concentration distribution in primary clarifiers. *Canadian Journal of Civil Engineering* **12** (3), 454–463. doi:10.1139/l85-053.

Adams, E. W. & Rodi, W. 1990 Modeling flow and mixing in sedimentation tanks. *Journal of Hydraulic Engineering* **116** (7), 895–913. doi:10.1061/(ASCE)0733-9429(1990)116:7(895).

Alarie, R. L., Farquhar, G. J. & McBean, E. A. 1980 Simulation modeling of primary clarifiers. *Journal of the Environmental Engineering Division* **106** (2), 293–309.

Al-Sammarraee, M., Chan, A., Salim, S. M. & Mahabaleswar, U. S. 2009 Large-eddy simulations of particle sedimentation in a

longitudinal sedimentation basin of a water treatment plant. Part I: particle settling performance. *Chemical Engineering Journal* **152** (2–3), 307–314. doi:10.1016/j.cej.2009.04.062.

Amini, E., Mehrnia, M., Mousavi, M. & Mostoufi, N. 2013 Experimental study and computational fluid dynamics simulation of a full-scale membrane bioreactor for municipal wastewater treatment application. *Industrial & Engineering Chemistry Research* **52** (29), 9930–9939. doi:10.1021/ie400632y.

ANSYS 2016 *ANSYS Fluent Theory Guide*. ANSYS, Inc, USA.

Applegate, C. S., Schneider, J. J. & Keller, J. 2010 Comparison of primary clarifier performance, baffled versus conventional feedwell at the buffalo sewer authority. In: *Proceedings of the WEFTEC 83th Annual Technical Exhibition and Conference*, New Orleans, LA. doi:10.2175/193864710798194201.

Asgharzadeh, H., Firoozabadi, B. & Afshin, H. 2011 Experimental investigation of effects of baffle configurations on the performance of a secondary sedimentation tank. *Scientia Iranica* **18** (4B), 938–949.

Bachis, G., Maruéjouls, T., Tik, S., Amerlinck, Y., Melcer, H., Nopens, I., Lessard, P. & Vanrolleghem, P. A. 2015 Modelling and characterization of primary settlers in view of whole plant and resource recovery modelling. *Water Science & Technology* **72** (12), 2251–2261. doi:10.2166/wst.2015.455.

Balemans, S. 2014 *Towards Improved Secondary Settling Tanks by Means of Computational Fluid Dynamics*. Master thesis, Ghent University.

Bridgeman, J., Jefferson, B. & Parsons, S. A. 2009 Computational fluid dynamics modelling of flocculation in water treatment: a review. *Engineering Applications of Computational Fluids Mechanics* **3**, 220–241. doi:10.1080/19942060.2009.11015267.

Camp, T. R. 1946 Sedimentation and the design of settling tanks. *Transactions of the American Society of Civil Engineer* **111** (1), 895–936.

Carbone, M., Garofalo, G. & Piro, P. 2014 Comparison between CFD and surface overflow rate models to predict particulate matter separation in unit operations for combined sewer overflows. *Journal of Environmental Engineering* **140**, 411–414. doi:10.1061/(ASCE)EE.1943-7870.0000857.

Celik, I., Rodi, W. & Stamou, A. 1985 Prediction of hydrodynamic characteristics of rectangular settling tanks. In: *Proceedings of the International Symposium on Refined Flow Modelling and Turbulence Measurements*. Iowa City, Iowa.

Cloete, S. & Amini, S. 2016 The dense discrete phase model for simulation of bubbling fluidized beds: validation and verification. In: *Proceedings 9th International Conference on Multiphase Flow*. Firenze, Italy.

Cloete, S., Johansen, S. T., Braun, M., Popoff, B. & Amini, S. 2011 Evaluation of a lagrangian discrete phase modeling approach for application to industrial scale bubbling fluidized beds. In: *Proceedings of the 10th International Conference on Circulating Fluidized Beds and Fluidization Technology*. Sun River, Oregon, USA.

Cloete, S., Johansen, T. S. & Amini, S. 2012 Performance Evaluation of a complete lagrangian KTGF approach for dilute granular flow modelling. *Powder Technology* **226**, 43–52. doi:10.1016/j.powtec.2012.04.010.

Das, S., Bai, H., Ch, W., Kao, J.-H., Barney, B., Kidd, M. & Kuettel, M. 2016 Improving the performance of industrial clarifiers using three-dimensional computational fluid dynamics. *Engineering Applications of Computational Fluid Mechanics* **10** (1), 130–144. doi:10.1080/19942060.2015.1121518.

De Clercq, B. 2003 *Computational Fluid Dynamics of Settling Tanks: Development of Experiments and Rheological, Settling, and Scraper Submodels*. Ph.D. thesis, Ghent University.

Devantier, B. A. & Larock, B. E. 1986 Modelling a recirculating density-driven turbulent flow. *International Journal for Numerical Methods in Fluids* **6** (4), 241–253. doi:10.1002/fld.1650060406.

Dobbins, W. E. 1944 Effect of turbulence on sedimentation. *Transactions of the American Society of Civil Engineers* **109**, 629–656.

Droste, R. L. 1997 *Theory and Practice of Water and Wastewater Treatment*. John Wiley & Sons, New York.

Dufresne, M., Vazquez, J., Terfous, A. & Ghernaim, A. 2009 Experimental Investigation and CFD Modelling of flow, sedimentation, and solids separation in a combined sewer detention tank. *Computers and Fluids* **38** (5), 1042–1049. doi:10.1016/j.compfluid.2008.01.011.

Ekmekçi, H. B. 2015 *Modification of A Computational Fluid Dynamics Model (ANSYS-FLUENT) for the Purpose of River Flow and Sediment Transport Modeling*. Master's thesis, İzmir Institute of Technology, Izmir.

Esping, D., Shaposka, H., Wahlberg, E., Ifft, J. & McCorquodale, J. A. 2012 Optimizing primary sedimentation and wet weather flow treatment using CFD modeling. In: *Proceedings of the WEFTEC 85th Annual Technical Exhibition and Conference*. doi:10.2175/193864712811709517.

Fan, L., Xu, N., Ke, X. & Shi, H. 2007 Numerical simulation of secondary sedimentation tank for urban wastewater. *Journal of the Chinese Institute of Chemical Engineers* **38** (5–6), 425–433. doi:10.1016/j.jcice.2007.06.006.

Gao, H. & Stenstrom, M. K. 2017 Computational fluid dynamics applied to secondary clarifier analysis. In: *Proceedings of World Environmental and Water Resources Congress 2017*. Sacramento, CA. doi:10.1061/9780784480632.023.

Gao, H. & Stenstrom, M. K. 2018 Evaluation of three turbulence models in predicting of the hydrodynamics of a secondary sedimentation tank. *Water Research* **143**, 445–456. doi:10.1016/j.watres.2018.06.0670043-1354.

Gao, H. & Stenstrom, M. K. 2019 Development and applications in CFD modeling for secondary settling tanks over the last three decades: a review. *Water Environmental Research* **92** (6), 796–820. doi:10.1002/WER.1279.

Garofalo, G. 2012 *Physical and Computational Fluid Dynamics Modeling of Unit Operations Under Transient Hydraulic Loadings*. DPH Thesis, University of Florida.

Gernaey, K. V. & Vanrolleghem, P. A. 2001 Modeling of reactive primary clarifier. *Water Science and Technology* **43** (7), 73–81. doi:10.2166/wst.2001.0393.

Ghawi, A. G. & Kriš, J. 2011 Improvement performance of secondary clarifiers by a computational fluid dynamics

model. *Slovak Journal of Civil Engineering* **XIX** (4), 1–11. doi:10.2478/v10189-011-0017-9.

Ghawi, A. G. & Kriš, J. 2012 A computational fluid dynamics model of flow and settling in sedimentation tanks. In: *Applied Computational Fluid Dynamics* (H. W. Oh, ed.). doi:10.5772/27160.

Gidaspow, D., Bezburuah, R. & Ding, J. 1992 Hydrodynamics of circulating fluidized beds: kinetic theory approach. In: *Proceedings of 7th International Conference on Fluidization*. Australia.

Gong, M., Xanthos, S., Ramalingam, K., Fillos, J., Beckman, K., Deur, A. & McCorquodale, J. A. 2010 CFD Modeling of final settling tanks: ramping up from 2D to 3D. In: *Proceedings of the WEFTEC 83th Annual Technical Exhibition and Conference*. New Orleans, LA. doi:10.2175/193864710798208188.

Gong, M., Xanthos, S., Ramalingam, K., Fillos, J., Beckman, K., Deur, A. & McCorquodale, J. A. 2011 Development of a flocculation sub-model for a model based in rectangular settling tanks. *Water Science & Technology* **63** (2), 213–219. doi:10.2166/wst.2011.035.

Goula, A. M., Kostoglou, M., Karapantsios, T. D. & Zouboulis, A. I. 2008 A CFD methodology for the design of sedimentation tanks in potable water treatment. Case study: the influence of a feed flow control baffle. *Chemical Engineering Journal* **140**, 110–121. doi:10.1016/j.cej.2007.09.022.

Griborio, A. & McCorquodale, J. A. 2006 Optimum design of your center well: use of a CFD model to understand the balance between flocculation and improved hydrodynamics. In: *Proceedings of the WEFTEC 79th Annual Technical Exhibition and Conference*. Dallas, TX. doi:10.2175/193864706783710587.

Griborio, A., McCorquodale, J. A. & Rodriguez, J. A. 2014 CFD Modeling of Primary Clarifiers: The State-of-the-Art. In: *Proceedings of the WEFTEC 87th Annual Technical Exhibition and Conference*. New Orleans, LA. doi:10.2175/193864714815941540.

Guo, H., Ki, S. J., Oh, S., Kim, Y. M., Wang, S. & Kim, J. H. 2017 Numerical simulation of separation process for enhancing fine particle removal in tertiary sedimentation tank mounting adjustable baffle. *Chemical Engineering Science* **158**, 21–29. doi:10.1016/j.ces.2016.09.022.

Hazen, A. 1904 On sedimentation. *Transactions of ASCE* **53** (2), 45–71.

Imam, E., McCorquodale, J. A. & Bewtra, J. K. 1983 Numerical modeling of sedimentation tanks. *Journal of Hydraulic Engineering* **109** (12), 1740–1754. doi:10.1061/(ASCE)0733-9429(1983)109:12(1740).

Kim, H. S., Shin, M. S., Jang, D. S., Jung, S. H. & Jin, J. H. 2005 Study of flow characteristics in a secondary clarifier by numerical simulation and radioisotope tracer technique. *Applied Radiation and Isotopes* **63** (4), 519–526. doi:10.1016/j.apradiso.2005.03.016.

Kiss, K. 2012 On settling process in primary clarifiers. In: *2nd Conference of Junior Researchers in Civil Engineering*.

Klimanek, A., Adamczyk, W., Katelbach-Wozniak, A., Wecel, G. & Szlek, A. 2015 Towards a hybrid Eulerian–Lagrangian CFD modeling of coal gasification in a circulating fluidized bed reactor. *Fuel* **152**, 131–137. doi:10.1016/j.fuel.2014.10.058.

Kriss, J. & Ghawi, A. H. 2008 Study the effect of temperature on sedimentation tanks performance. In: *Proceedings of XXth Jubilee-National, VIIIth International Scientific and Technical Conference, Water Supply and Water Quality*. Poland.

Li, X., Zhai, X., Chu, H. P. & Zhang, J. 2008 Characterization of the flocculation process from the evolution of particle size distributions. *Journal of Environmental Engineering* **134** (5), 369–375. doi:10.1061/(ASCE)0733-9372(2008)134:5(369).

Liu, X. & García, M. H. 2007 *Numerical Modeling of the Calumet Water Reclamation Plant (CWRP) Primary Settling Tanks*. Hydraulic Engineering Series. Rep. No. 80, Dept. of Civil and Environmental Engineering, University of Illinois, Urbana-Champaign.

Liu, X. & García, M. H. 2011 Computational fluid dynamics modeling for the design of large primary settling tanks. *Journal of Hydraulic Engineering* **137** (3), 343–355. doi:10.1061/(ASCE)HY.1943-7900.0000313.

Lun, C. K. K., Savage, S. B., Jeffrey, D. J. & Chepurniy, N. 1984 Kinetic theories for granular flow: inelastic particles in Coutte flow and slightly inelastic particles in a general flow field. *Journal of Fluid Mechanics* **140**, 223–256. doi:10.1017/S0022112084000586.

Manninen, M., Taivassalo, V. & Kallio, S. 1996 *On the Mixture Model for Multiphase Flow*. Espoo 1996, Technical Research Centre of Finland, VTT Publications 288.

McCorquodale, A., Griborio, A. & Georgiou, I. 2005 A Public Domain Settling Tank Model. In: *Proceedings of the WEFTEC 78th Annual Technical Exhibition and Conference*. Washington, DC. doi:10.2175/193864705783865668.

Nguyen, T. V., Farrow, J. B., Smith, J. & Fawell, P. D. 2012 Design and development of a novel thickener feedwell using computational fluid dynamics. *The Journal of The Southern African Institute of Mining and Metallurgy* **112** (11), 939–948.

Njobuenwu, D. O., Fairweather, M. & Yao, J. 2013 Coupled RANS–LPT modelling of dilute, particle-laden flow in a duct with a 90° bend. *International Journal of Multiphase Flow* **50**, 71–88. doi:10.1016/j.ijmultiphaseflow.2012.10.009.

Ogawa, S., Umemura, A. & Oshima, N. 1980 On the equations of fully fluidized granular materials. *Journal of Applied Mathematics and Physic* **31**, 483–493. doi:10.1007/BF01590859.

Paraskevas, P. A., Kolokithas, G. & Lekkas, T. D. 1993 A complete dynamic model of primary sedimentation. *Environmental Technology* **14** (11), 1037–1046. doi:10.1080/09593339309385380.

Patel, N., Patel, N. & Barve, J. 2016 Modelling, simulation and validation of continuous sedimentation process. In: *Proceedings of Indian Control Conference*. Hyderabad, India. doi:10.1109/INDIANCC.2016.7441164.

Patziger, M. & Kiss, K. 2015 Analysis of suspended solids transport process in primary settling tanks. *Water Science & Technology* **72** (1), 1–8. doi:10.2166/wst.2015.168.

Patziger, M., Günthert, F. W., Jardin, N., Kainz, H. & Londong, J. 2016 On the design and operation of primary settling tanks in state-of-the-art wastewater treatment and water resources recovery. *Water Science & Technology* **74** (9), 2060–2067. doi:10.2166/wst.2016.349.

Rameshwaran, P., Naden, P., Wilson, C. A. M. E., Malki, R., Shukla, D. R. & Shiono, K. 2013 Inter-comparison and validation of computational fluid dynamics codes in two-stage meandering channel flows. *Applied Mathematical Modelling* **37** (20–21), 8652–8672. doi:10.1016/j.apm.2013.07.016.

Ramin, E., Wagner, D. S., Yde, L., Binning, P. J., Rasmussen, M. R., Mikkelsen, P. S. & Plosz, B. G. 2014 A new settling velocity model to describe secondary sedimentation. *Water Research* **66**, 447–458. doi:10.1016/j.watres.2014.08.034.

Razmi, A., Firoozabadi, B. & Ahmadi, G. 2009 Experimental and numerical approach to enlargement of performance of primary settling tanks. *Journal of Applied Fluid Mechanics* **2** (1), 1–12. doi:10.36884/jafm.2.01.11850.

Rodi, W. 2017 *Turbulence Models and Their Application in Hydraulics: A State-of-the-art Review*, 3rd edn. CRC Press. doi:10.1201/9780203734896.

Rostami, F., Shahrokhi, M., Md Said, M. A., Abdullah, R. & Syafalni 2011 Numerical modeling on inlet aperture effects on flow pattern in primary settling tanks. *Applied Mathematical Modelling* **35** (6), 3012–3020. doi:10.1016/j.apm.2010.12.007.

Roy, S., Sai, P. S. T. & Jayanti, S. 2014 Numerical simulation of the hydrodynamics of a liquid solid circulating fluidized bed. *Powder Technology* **251**, 61–70. doi:10.1016/j.powtec.2013.10.033.

Samstag, R. W., Dittmar, D. F., Vitasovic, Z. & McCorquodale, J. A. 1992 Underflow geometry in secondary sedimentation. *Water Environment Research* **64** (3), 204–212. doi:10.2175/WER.64.3.3.

Samstag, R. W., Ducoste, J. J., Griborio, A., Nopens, I., Batstone, D. J., Wicks, J. D., Saunders, S., Wicklein, E. A., Kenny, G. & Laurent, J. 2016 CFD for wastewater treatment: an overview. *Water Science & Technology* **74** (3), 549–563. doi:10.2166/wst.2016.249.

Schaeffer, D. G. 1987 Instability in the evolution equations describing incompressible granular flow. *Journal of Differential Equations* **66**, 19–50. doi:10.1016/0022-0396(87)90038-6.

Shahrokhi, M., Rostami, F., Md Said, M. A. & Syafalni 2011 Numerical simulation of influence of inlet configuration on flow pattern in primary rectangular sedimentation tanks. *World Applied Sciences Journal* **15** (7), 1024–1031.

Shahrokhi, M., Rostami, F., Md Said, M. A., Sabbagh Yazdi, S. R. & Syafalni 2012 The effect of number of baffles on the improvement efficiency of primary sedimentation tanks. *Applied Mathematical Modelling* **36**, 3725–3735. doi:10.1016/j.apm.2011.11.001.

Shahrokhi, M., Rostami, F., Md Said, M. A., Sabbagh Yazdi, S. R. & Syafalni, S. 2013 Computational investigations of baffle configuration effects on the performance of primary sedimentation tanks. *Water and Environment Journal* **27** (4), 484–494. doi:10.1111/j.1747-6593.2012.00367.x.

Stamou, A. I. 1991 On the prediction of flow and mixing in settling tanks using a curvature-modified k-ε model. *Applied Mathematical Modelling* **15**, 351–358. doi:10.1016/0307-904X(91)90060-3.

Stamou, A. I. 1995 Modelling of settling tanks – a critical review. *WIT Transactions on Ecology and the Environment* **7**, 305–312.

Stamou, A. I. 2008 Improving the hydraulic efficiency of water process tanks using CFD models. *Chemical Engineering and Processing* **47** (8), 1179–1189. doi:10.1016/j.cep.2007.02.033.

Stamou, A. I., Adams, E. W. & Rodi, W. 1989 Numerical modeling of flow and settling in primary rectangular clarifiers. *Journal of Hydraulic Research* **27** (5), 665–682. doi:10.1080/00221688909499117.

Tamayol, A. & Firoozabadi, B. 2006 Effects of turbulent models and baffle position on the hydrodynamics of settling tanks. *Scientia Iranica* **13** (3), 255–260.

Tamayol, A., Firoozabadi, B. & Ahmadi, G. 2008 Effects of inlet position and baffle configuration on hydraulic performance of primary settling tanks. *Journal of Hydraulic Engineering* **134** (7), 1004–1009. doi:10.1061/(ASCE)0733-9429(2008)134:7(1004).

Tarpagkou, R. & Pantokratoras, A. 2014 The influence of lamellar settler in sedimentation tanks for potable water treatment – A computational fluid dynamic study. *Powder Technology* **268** (1), 139–149. doi:10.1016/j.powtec.2014.08.030.

Tarpagkou, R., Pantokratoras, A. & Papadakis, N. 2013 The influence on the flow field and performance of a sedimentation tank for potable water treatment due to low (winter) and high (summer) temperatures. In: *Proceedings of the 13th International Conference on Environmental Science and Technology*. Atenas.

Tebbutt, T. H. & Christoulas, D. G. 1975 Performance relationships for primary sedimentation. *Water Research* **9** (4), 347–356. doi:10.1016/0043-1354(75)90180-3.

Torfs, E., Marti, M., Locatelli, F., Balemans, S., Bürger, R., Diehl, S., Laurent, J., Vanrolleghem, P. A., François, P. & Nopens, I. 2017 Concentration-driven models revisited: towards a unified framework to model settling tanks in water resource recovery facilities. *Water Science & Technology* **75** (3), 539–551. doi:10. 2166/wst.2016.485.

Wang, X. L., Li, T., Lang, J., Zhou, S. S., Zhang, L. L. & Chen, M. X. 2010 Numerical analysis of solid-liquid two-phase flow on sandstone wastewater of hydropower stations in a rectangular sedimentation tank. *Industrial and Engineering Chemistry Research* **49** (22), 11714–11723. doi:10.1021/ie901993t.

Water Environment Federation. 2005 *Clarifier Design. Manual of Practice No. FD-8*. McGraw-Hill, New York.

Weiss, M., Plósz, B. G., Essemiani, K. & Meinhold, J. 2007 Suction-lift sludge removal and non-Newtonian flow behavior in circular secondary clarifiers: numerical modelling and measurements. *Chemical Engineering Journal* **132** (1–3), 241–255. doi:10.1016/j.cej.2007.01.004.

Wicklein, E. A. & Samstag, R. W. 2009 Comparing commercial and transport CFD models for secondary sedimentation. In: *Proceedings of the 82nd WEFTEC Exhibition and Conference*. Orlando, FL. doi:10.2175/193864709793952765.

Wicklein, E., Batstone, D. J., Ducoste, J., Laurent, J., Griborio, A., Wicks, J. & Nopens, I. 2015 Good modelling practice in applying computational fluid dynamics for WWTP modelling. *Water Science and Technology* **73** (5), 969–982. doi:10.2166/wst.2015.565.

Xanthos, S., Gong, M., Ramalingam, K., Fillos, J., Deur, A., Beckmann, K. & McCorquodale, J. A. 2011 Performance assessment of secondary settling tanks using CFD modeling. *Water Resources Management* **25** (4), 1169–1182. doi:10.1007/s11269-010-9620-1.

Yeoh, G. H. & Tu, J. 2009 *Computational Techniques for Multiphase Flows*, 1st edn. Elsevier, UK.

Ying, G. & Sansalone, J. 2011 Gravitational settling velocity regimes for heterodisperse urban drainage particulate matter. *Journal of Environmental Engineering* **137** (1), 15–27. doi:10.1061/(ASCE)EE.1943-7870.0000298.

Yu, L., Ma, J., Frear, C., Zhao, Q., Dillon, R., Li, X. & Chen, S. 2013 Multiphase modeling of settling and suspension in anaerobic digester. *Applied Energy* **111**, 28–39. doi:10.1016/j.apenergy.2013.04.073.

Zhang, D. 2014 *Optimize Sedimentation Tank and lab Flocculation Unit by CFD*. Master thesis, Norwegian University of Life Sciences.

Zhang, A. 2017 *CFD Modeling and Optimization of Primary Sedimentation Tank. Particularly Focus on Inlet Zone and Inlet Flow*. Master thesis, KTK Stockholm, Sweden.

Zhang, Q., Wang, S., Lu, H., Liu, G., Wang, S. & Zhao, G. 2017 A coupled Eulerian fluid phase-Eulerian solids phase-Lagrangian discrete particles hybrid model applied to gas-solids bubbling fluidized beds. *Powder Technology* **315**, 385–397. doi:10.1016/j.powtec.2017.04.024.

Zhou, S. & McCorquodale, J. A. 1992 Mathematical Modelling of a circular clarifier. *Canadian Journal of Civil Engineering* **19** (3), 365–374. doi:10.1139/l92-044.

Zhou, S., McCorquodale, J. A. & Godo, A. M. 1994 Short circuiting and density interface in primary clarifiers. *Journal of Hydraulic Engineering* **120**, 1060–1080. doi:10.1061/(ASCE)0733-9429(1994)120:9(1060).

Zhou, S., McCorquodale, J. A., Richardson, J. & Wilson, T. 2005 State of the art clarifier modelling technology-Part II. In: *Proceedings of the WEFTEC 78th Annual Technical Exhibition and Conference*. Washington, DC. doi:10.2175/193864705783815131.

Zhou, Q., Wang, C., Wang, H. & Wang, J. 2016 Eulerian–Lagrangian study of dense liquid–solid flow in an industrial-scale cylindrical hydrocyclone. *International Journal of Mineral Processing* **151**, 40–50. doi:10.1016/j.minpro.2016.04.005.

Zhu, G., Zhang, Y., Ren, J., Qiu, T. & Wang, T. 2012 Flow simulation and analysis in a vertical-flow sedimentation tank. *Energy Procedia* **16**, 197–202. doi:10.1016/j.egypro.2012.01.033.

First received 31 December 2020; accepted in revised form 12 March 2021. Available online 23 March 2021